Proceedings of the 2005 IEEE
International Conference on Robotics and Automation
Barcelona, Spain, April 2005

Multi-Axis SMA Actuator Array for Driving Anthropomorphic Robot Hand

Kyu-Jin Cho, and Harry Asada

d'Arbeloff Laboratory for Information Systems and Technology
Department of Mechanical Engineering
Massachusetts Institute of Technology
Cambridge, MA 02139, USA
kyujin@mit.edu, asada@mit.edu

***Abstract*— A novel multi-axis Shape Memory Alloy (SMA) array actuator has been developed for driving five-fingered anthropomorphic robot hand. The new actuator array uses Segmented Binary Control (SBC), which controls the SMA wires segment by segment in a digital manner. Normally, SMA wires are hard to control and require nonlinear controllers to control each wire. SBC simplifies the control of SMA wire but increases the complexity of the design and the number of control loops. A multi-axis segmentation theory has been developed to reduce the design complexity and the number of control loops by reducing the number of segments. Segmentation architecture of an actuator array is designed for five-fingered robotic hand that performs fourteen different postures. The segmentation architecture is implemented with ten SMA wires sandwiched between a layer of thermoelectric modules embedded on a printed circuit board and a layer of acrylic substrate board with grooves. Initial results of the segmented binary controlled SMA wire are verified with minimum segment architecture of a single axis.**

I. Introduction

High degree of freedom (DOF) is one of the main factors that distinguish anthropomorphic robot hands from simple manipulators. Anthropomorphic robot hands with high DOF are built to provide dexterity similar to that of human hands [1]. Dexterous robotic hands built over the last two decades include articulated hands by Salisbury

[2], Utah/MIT hand [3], Standford/JPL hand [4] Belgrade/USC hand [5], DIST hand [6] and Gifu hand [7]. Number of actuators used in these hands ranges from 9 to 32 with 3 to 5 fingers [1]. Most of these works use electric motors for driving the hands.

Although these robotic hands have high DOF, recently developed humanoid robots have small DOF assigned to their hands. Sony's Qrio [8] has 5 DOF for each hand with 38 DOF for the whole system, and Honda's Asimo [9] and Fujitsu's HOAP-2[10] has 1 DOF for each hand with 24 and 25 DOF for the whole system, respectively. The size and weight of the actuators limit the DOF of robotic hands that can be equipped in humanoid robots. Therefore, robotic hands for humanoid robots can benefit from compact and easy-to-control actuators with large number of axis.

In this paper, a novel compact multi-axis shape memory alloy (SMA) actuator array for driving five-fingered anthropomorphic robot hand is presented. The new actuator array uses Segmented Binary Control (SBC) [18], which controls the SMA wires segment by segment in a digital manner. This Segmented Binary Control of SMA wires resembles a biological muscle producing a resultant displacement as the addition of all the displacements created by the short muscle fibers controlled as finite-state machines [19]. In the following, a brief description of the SBC is first provided along with a segmentation architecture that enables the reduction of number of segments. Multi-axis segmentation theory is presented which defines the coupling coefficient matrix that is used as the basic tool for designing the segmentation architecture. And then, design procedure for a ten-axis actuator array for driving a robotic hand that can perform fourteen different postures is presented. The designed segmentation architecture is implemented with ten SMA wires sandwiched between a layer of thermoelectric modules embedded on a printed circuit board and a layer of substrate board with grooves. The developed SMA actuator array has ten axes and each axis can produce maximum force of 1.25kgf and a maximum displacement of 7.2mm. Initial results of the segmented binary controlled SMA wire are verified using an experimental setup with four segments that can produce fifteen-step displacements.

II. Segmented Binary Control

Traditional SMA drive systems consist of heating the entire length of wire with electric current and cooling with natural or forced convection. Fig. 1-(a) shows a schematic of this system. The entire SMA wire is controlled as a single process. An alternative to these methods, Segmented Binary Control, has been proposed by H. Asada et al [18] to control SMA wire segment-by-segment separately with a simple control law for each segment, as shown in Fig. 1-(b). This method uses basic characteristics of SMA wires, which makes displacement at one end of the wire equal to the summation of individual displacements contributed by all the segments. Therefore, we do not have to control the

This material is based upon work supported by the National Science Foundation under Grant No. IIS-0413242.

strain or phase of the wire as a whole, but can generate the same total displacement by heating or cooling local segments of the wire in a binary manner. The advantage is that pushing the phase of specific segments to all austenite phase or all martensite phase, rather than keeping the phase of the entire wire somewhere between the two extremes, would make the SMA wire insensitive to complex nonlinearity and hysteresis.

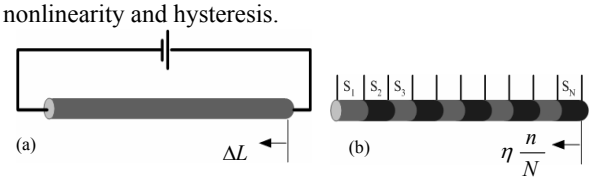

Fig. 1. (a) Traditional SMA heating method and (b) Segmented Binary Control. N is the number of segments and n is the number of austenite segments [18]

One drawback of SBC is increased number of control loops and drive system. Although each control loop regulating the phase of an individual segment is rather simple, many loops are needed. SBC may not be useful nor can practically be justifiable, if it entails many feedback loops for controlling individual segments of each axis.

Since the SMA wire is digitized under SBC, the resolution of the output displacement depends on the number of segments. If the entire wire is segmented equally in length, as in the case of Fig. 1-(b), the length of each segment is given by $\ell = L/N$, where L is the length of the wire and N is the number of segments having an equal length. The resolution is then $\eta = \bar{\varepsilon} \cdot \ell$, where $\bar{\varepsilon}$ is target strain, typically 4%. This uniform segmentation turns out to be least efficient. It is in fact redundant. If N is given by $N = \sum_{i=0}^{b} 2^i$, total of b control loops, instead of N, can provide the same resolution η. As shown in Fig. 3, the length of each segment is set to be powers of two, i.e. 1, 2, 4, 8, …, of the unit length ℓ and an independent control loop is assigned to each segment with a different unit length. Then the b control loops can generate any number of units turned to be in either austenite or martensite state.

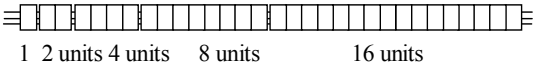

Fig. 2. Minimum segmentation of single axis

With this segmentation, the number of control loops can be minimized for a single axis SMA actuator. When we consider M-axis actuators, the number of control loops becomes M times b, and that is too many to practically implement. The authors have proposed an effective method of reducing the control loops for multi-axis SMA actuators [19]. As illustrated in Fig. 3, M-axes of SMA wires are laid on a two-dimensional array of local heating and cooling units. Note that this two-dimensional array of units is segmented not only in the longitudinal direction of each bundle of SMA wires but also in the transverse direction. Therefore adjacent SMA wires lay on the same segment are heated or cooled at the same time for that particular portion of the wires. This, of course, reduces independence of the adjacent SMA wires to a certain degree, but on the other hand generates a coordinated movement among them. It is also important to note that with this two-dimensional segmentation the number of control loops is significantly reduced.

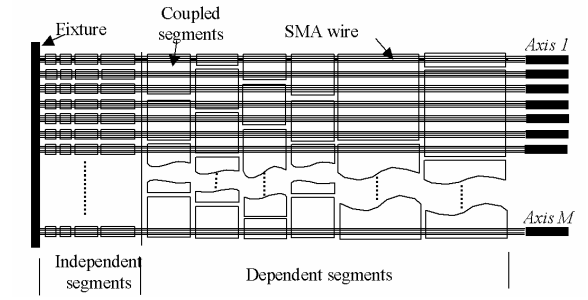

Fig. 3. Two-dimensional segmentation of multi-axis SMA actuator system on Peltier pellet bed[19]

III. Multi-Axis Segmentation Theory

Based on the two-dimensional segmentation architecture, fundamental properties of multi-axis coordination using SBC will be analyzed in this section. Consider a subset of actuator axes A_m, as shown in Fig. 4. The subset consists of m, $1 \le m \le M$, actuator axes with an equal total length:

$$A_m = \{i_j \,|\, 1 \le i_1 < i_2 < \cdots < i_m \le M\} \tag{1}$$

If these m axes are to generate "similar" output displacements, $y_i(t), \forall i \in A_M$, they should be generated with some coupled segments combined with independent segments. The goal of the analysis is to quantify the "similarity" of output trajectories and find the coupled segments of a proper length that can generate the "similar" part of the trajectories.

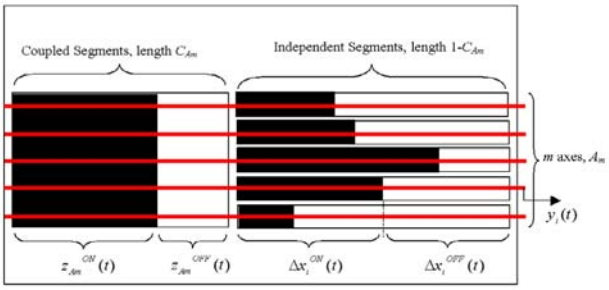

Fig. 4 Coupled and independent segments of m axis array

Fig. 5-(a) illustrates trajectories of a subset of actuators A_m defined over time interval T_I:

$$0 \le y_i(t) \le 1, \quad \text{for } \forall t \in T_I, \forall i \in A_m \tag{2}$$

The dynamic range of these trajectories stays in a certain middle range, as shown by the shaded area in Fig. 5-(b). The figure also indicates the normalized length of the actuator material at ON-state, $x_i^{ON}(t)$, as well as the one of

OFF-state, $x_i^{OFF}(t)$, corresponding to the output trajectories, $x_i^{ON}(t) = y_i(t)$. The height below the shaded area, given by $\ell^{ON} = \underset{i \in Am}{Min}\, x_i^{ON}(t)$, implies that all the m actuators have at least ℓ^{ON} length of ON-state, while the one above the shaded area, given by $\ell^{OFF} = \underset{i \in Am}{Min}\, x_i^{OFF}(t)$, indicates that all the m actuators have at lest ℓ^{OFF} length of OFF-state. In other words, all the m actuators share $\ell^{ON} + \ell^{OFF}$ length of ON/OFF states. Fig. 5-(c) shows the profile of the sum of these lengths $\ell^{ON} + \ell^{OFF}$ and its lower bound for the entire time span:

$$C_{Am} = \underset{t \in T_I}{Min}\,[\underset{i \in Am}{Min}\, x_i^{ON}(t) + \underset{i \in Am}{Min}\, x_i^{OFF}(t)] \tag{3}$$

The lower bound C_{Am}, shown by the dot-and-dash line in the figure, represents how much the subset of axes A_m can be controlled together for the entire trajectories with a block of coupled segments. The coefficient C_{Am}, referred to as a *Coupling Coefficient* of order m, plays the major role in determining how much the multi-axis segments can be lumped together. Now, the following theorem constitutes the principle of multi-axis segmentation.

Theorem Let $x_i^{ON}(t)$ and $x_i^{OFF}(t)$ be, respectively, the lengths of ON-state segments and OFF-state segments that generate a given trajectory of the *i-th* actuator axis. Let A_m be a subset of m actuator axes and $z_{Am}^{ON}(t)$ and $z_{Am}^{OFF}(t)$ be, respectively, the lengths of ON state and OFF state of coupled segments across the m axes in A_m. If the total length of the coupled segments is no larger than the coupling coefficient C_{Am},

$$\begin{aligned} & z_{Am}^{ON}(t) + z_{Am}^{OFF}(t) \le C_{Am} \\ & = \underset{t \in T_I}{Min}\,[\underset{i \in Am}{Min}\, x_i^{ON}(t) + \underset{i \in Am}{Min}\, x_i^{OFF}(t)], \quad \forall t \in T_I \end{aligned} \tag{4}$$

then the segment lengths, $x_i^{ON}(t)$ and $x_i^{OFF}(t)$, can be generated by a combination of the coupled segments $z_{Am}^{ON}(t)$ and $z_{Am}^{OFF}(t)$ and independent segments such that:

$$\begin{aligned} & x_i^{ON}(t) = z_{Am}^{ON}(t) + \Delta x_i^{ON}(t), \\ & x_i^{OFF}(t) = z_{Am}^{OFF}(t) + \Delta x_i^{OFF}(t), \quad \forall t \in T_I, \forall i \in A_m \end{aligned} \tag{5}$$

where $\Delta x_i^{ON}(t)$ and $\Delta x_i^{OFF}(t)$ are, respectively, the lengths of the independent segments at ON state and OFF state. The total length of the two is no larger than 1- C_{Am},

$$0 \le \Delta x_i^{ON}(t) + \Delta x_i^{OFF}(t) \le 1 - C_{Am}, \quad \forall i \in A_m \tag{6}$$

Hence, the independent segments can generate the given m trajectories although the coupled segments of length less than C_{Am} are lumped together.

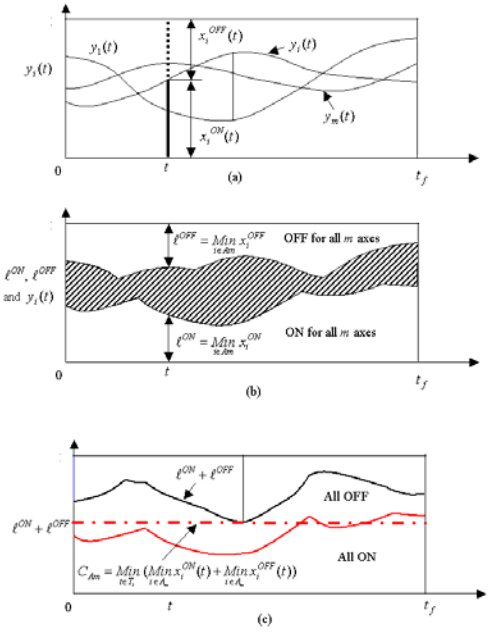

Fig. 5. Trajectories of m axes (a), all On and OFF states for all the m axes (b), and the common segments (c)

The above theorem is used for designing the segmentation architecture of multi-axis actuator array.

IV. Application to an Anthropomorphic Robot Hand

The design concept of multi-axis actuator array with two-dimensional segmentation architecture is applied to an anthropomorphic robot hand. A single human hand has 19 joints at the five fingers alone. Despite numerous degrees of freedom, many of them are coupled. Such coupled motion can be generated effectively with use of multi-axis segmented binary control.

Behavior of human fingers has been studied in the robotics and biomechanics communities for years. Okada [13] and Cutkosky [14] characterized human grasp and manipulative behavior and classified various poses into seven groups. More recently, human finger postures have been studied extensively in the field of human-computer interaction (HCI) [15]-[17]. To better understand hand gestures from visual images and other sensor data, anatomical and kinesiological constraints among multiple joint axes are used for eliminating unnatural poses and physiologically infeasible poses [16]. Such constraints greatly reduce the search space. Like-wise, the reduction in the space of natural poses helps us construct a multi-axis actuator array for driving an anthropomorphic robot hand.

Fig. 6 shows fourteen different postures, ranging from open, survey, and envelope to pinch grips and write grip. For these postures, finger joint angles can be derived. These joint angles are transformed into displacements of the actuators driving the individual joints. To implement segmented binary control, the displacements must be discretized with resolution equal to the resolution of the

actuator. The resolution of the actuator is the output displacement that can be produced by the smallest segment. The discretized displacements are then normalized and used to design segmentation.

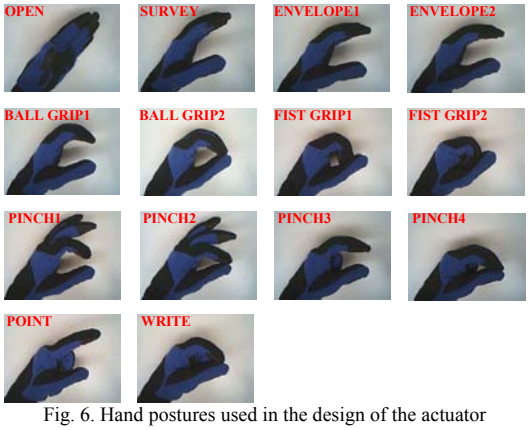

Fig. 6. Hand postures used in the design of the actuator

SMA actuators with length equal to N smallest discrete segments drive each finger having a maximum bending angle of α_i. The smallest actuator segment can produce an output displacement of η. Angle θ_i of the *i-th* finger joint is transformed into normalized displacement y_i of the actuator axis i, using the following parameters:

$$y_i = \frac{N \cdot \eta}{\alpha_i} \theta_i \tag{7}$$

Note that $N \cdot \eta$ is the maximum output displacement that each axis can produce.

We have chosen to build array actuators consisting of five *30 mm* segments per axis, with a maximum joint bending angle of 90°; hence $N=5$ and α =90°. The displacements are quantized into five levels, and normalized by the maximum output displacement. Quantized and normalized values of the actuator displacements, $y_i(\theta_i)$, are directly derived from the defined joint angles as follows.

$$y_i(\theta_i) = \frac{k}{N} \quad \text{for} \quad k\frac{\alpha}{N} - \frac{1}{2}\frac{\alpha}{N} \le \theta_i < k\frac{\alpha}{N} + \frac{1}{2}\frac{\alpha}{N} \tag{8}$$

where k is an integer between 0 and 5.

Table 1 shows the discretized and normalized displacements used for segmentation design, where each column represents a specific hand posture and each row represents the displacements of each actuator.

After the displacements of the actuators has been normalized and discretized, the procedure for designing a multi-axis segmentation is three-fold: first the original M axis problem is divided into smaller uncoupled problems of fewer axes, second a gross segmentation layout is made for each uncoupled problem, and third the gross layout is fine-tuned to finalize the design.

TABLE 1. DISCRETIZED AND NORMALIZED DISPLACEMENTS USED FOR SEGMENTATION DESIGN

Actuator #	*Assigned Joint*	*Open*	*Survey*	*Envelope1*	*Envelope2*	*Ball1*	*Ball2*	*Fist1*	*Fist2*	*Pinch1*	*Pinch2*	*Pinch3*	*Pinch4*	*Point*	*Write*
1	*Thumb(DIP)*	0	0.2	0.2	0.4	0.4	0.6	0.8	1	0.4	0.4	0.4	0.4	1	0
2	*Thumb(MP)*	0	0.4	0.4	0.6	0.4	0.6	0.8	1	0.6	0.6	0.6	0.6	1	0.4
3	*Index(DIP)*	0	0.4	0.4	0.6	0.6	0.8	0.8	1	0.6	0.6	0.6	0.6	0	0.6
4	*Index(MP)*	0	0.2	0.4	0.6	0.2	0.4	0.8	1	0.6	0.8	0.6	0.8	0.4	0.6
5	*Middle(DIP)*	0	0.4	0.4	0.6	0.6	0.8	0.8	1	0.4	0.6	0.6	0.6	1	0.8
6	*Middle(MP)*	0	0.2	0.4	0.6	0.2	0.4	0.8	1	0.2	0.4	0.6	0.8	1	0.6
7	*Ring(DIP)*	0	0.4	0.4	0.6	0.6	0.8	0.8	1	0.2	0.4	1	1	1	1
8	*Ring(MP)*	0	0.2	0.4	0.6	0.2	0.4	0.8	1	0	0.2	1	1	1	1
9	*Pinkie(DIP)*	0	0.4	0.4	0.6	0.6	0.8	0.8	1	0	0.2	1	1	1	1

Step 1 Decoupling and Merger The coupling matrix is computed for the displacement data of the finger postures and is shown in Table 2. Axes 8 and 9 and axes 1 and 3 have been swapped. From the coupling coefficients, $C_{8,10}$ is 1, meaning the two actuators can be totally coupled. Hence axes 8 and 10 are merged. All other axes are coupled to some extent. Therefore, the ten-axis array cannot be divided into mutually independent subgroups.

TABLE 2 COUPLING MATRIX OF TEN-AXIS ACTUATOR ARRAY FOR HAND POSTURES SHOWN IN FIG. 10

	1	3	2	4	5	6	7	9	8	10
1	1	0	0.6	0.4	0.2	0.4	0	0	0	0
3	0	1	0	0.6	0	0	0	0	0	0
2	0.6	0	1	0.4	0.6	0.6	0.4	0.4	0.4	0.4
4	0.4	0.6	0.4	1	0.4	0.4	0.4	0.4	0.4	0.4
5	0.2	0	0.6	0.4	1	0.6	0.6	0.6	0.6	0.6
6	0.4	0	0.6	0.4	0.6	1	0.6	0.6	0.6	0.6
7	0	0	0.4	0.4	0.6	0.6	1	0.8	0.6	0.6
9	0	0	0.4	0.4	0.6	0.6	0.8	1	0.6	0.6
8	0	0	0.4	0.4	0.6	0.6	0.6	0.6	1	1
10	0	0	0.4	0.4	0.6	0.6	0.6	0.6	1	1

Step 2 Gross Segmentation All the possible, exclusive partitions of the axes involved in the subgroup were tried out, including the one leading to the minimum number of segments: Partition {{1}, {3}, {2, 4, 5, 6, 7, 8, 9, 10}}. Coupling coefficient of each partition is computed and the coupled segments were constructed. Since $C_{2,4\text{-}10}$ is 0.4, 40% of the actuator length can be lumped together as common segments.

Step3 Fine Segmentation After the initial gross segmentation design, a coupling matrix for the residual trajectories and the trajectories of the other axes not used for the gross segmentation in Step 2 was constructed. This process of constructing the coupling matrix, partitioning the actuators, and designing coupled segments is repeated until it cannot reduce the number of segments.

Fig. 7 shows the final segmentation design achieving the minimum number of segments. Twenty-one segments are used in the final design, which is 58% savings in the number of segments compared to when the actuators are not coupled

at all.

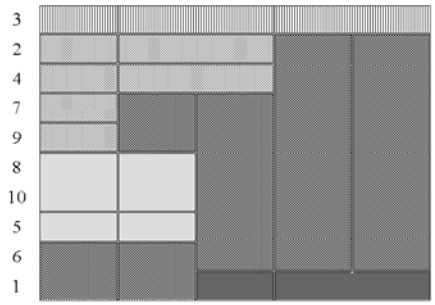

Fig. 7. Minimum segmentation design for ten-axis array actuators driving a robotic hand

V. Implementation Using Thermoelectric Modules

Thermoelectric modules are solid-state devices that convert electrical energy into a temperature gradient, known as the "Peltier effect". By changing the direction of the current flow, thermoelectric module can either heat or cool a surface. Thermoelectric modules are used to quickly heat and cool the segments of SMA actuators [18].

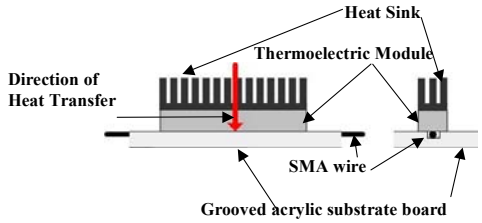

Fig. 8 Schematic of thermoelectric module on a grooved substrate board, driving a segment of SMA actuator wire

Cast acrylic boards with grooves of 7.6 mm width and 4 mm depth are used as a substrate board. Thermoelectric modules are attached on to the substrate board and the SMA wires are sandwiched between the TE module and the substrate board as shown in Fig. 8. When a current is applied to the thermoelectric device, it heats up, and in turn heats up the SMA wire. The groove maintains a gap between the TE module and the SMA wire sufficient for wire to move, but small enough for the heat to be transferred to the SMA wire from the TE module. Laser cutter(Epilog legend 24TT) is used to fabricate the acrylic substrate board in a single path.

A. Single Axis Setup and Experimental Result

Experimental setup has been built to verify the segmented binary control and a segmentation architecture shown in Fig. 2 that provides minimum number of segments for single axis case. The setup consists of 4 segments, each segment with a length of 15mm, 30mmm, 60mm and 120mm, equivalent to 1, 2, 4, 8 of the unit length of the module, as shown in Fig. 9. Each segment is heated to 120°C to turn On the actuator segment, and cooled to 30°C to turn Off the segment.

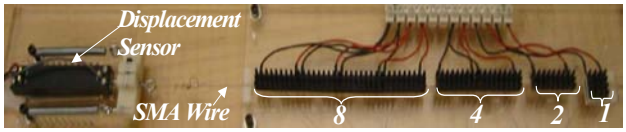

Fig. 9 Setup for single axis minimum segmentation

Fig. 10. shows the experimental results measured from the setup by turning on four segments in a sequence to create step displacement of one to fifteen. Note that this sequence is same as enumerating binary numbers, from 0001, 0010, 0011, 0010 to 1111 and assigning each digit to the equivalent segment. The segment is turned on when the equivalent digit is 1, and turned off when equivalent digit is 0. This sequence ideally creates step displacement from 0.72 mm to 15 * 0.72 mm. Displacement of the actuator wire is normalized by a displacement created by the smallest segment, and it is plotted against the length of the total heated thermoelectric device normalized by the length of the smallest TE module. Four different sets of data are plotted. 15 step outputs are created with just four segments of different sizes. The result shows a linear step output similar to a stepping motor.

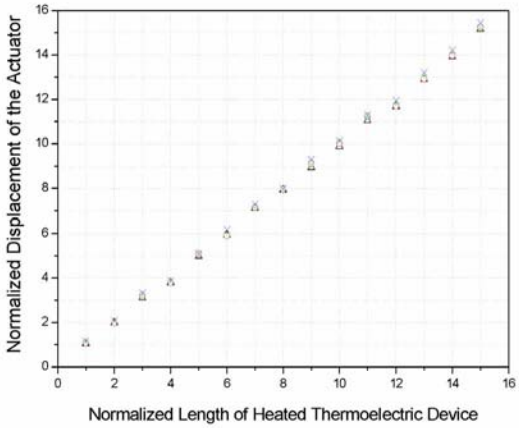

Fig. 10 Result of the unit step displacement experiment

B. Ten-Axis Actuator Array

The segmentation architecture of the Multi-Axis SMA Array Actuator designed in the previous section as shown in Fig. 7. is implemented. Fig. 11 shows the pictures of the prototype. The prototype consists of two layers, a substrate board layer and a TE module layer. As shown in Fig. 11(a), the substrate board layer with ten grooves is fabricated with a laser cutter and thermal adhesive tapes are placed to attach the TE modules. Crimped SMA wires are then placed in the grooves. Fig. 11(b) shows the layer with TE modules embedded onto a printed circuit board. This layer provides the electrical wiring for the TE modules and is attached with the substrate board. The layer has fifty 30mm by 5mm TE modules on it, and the segmentation architecture is implemented through electrical wiring and heat sink design. The SMA wires are sandwiched between the two layers,

and passes through the grooves. Fig. 11(c) shows the heat sinks placed on the TE modules. Note the architecture of the heat sinks is same as the segmentation architecture design of Fig. 7. The total number of control loops for this setup is 21, reduced from 50.

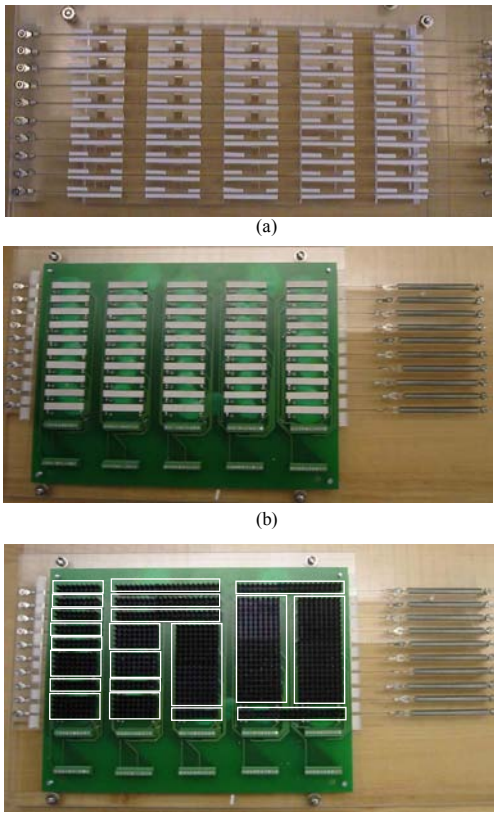

(a)

(b)

(c)

Fig. 11. Initial Prototype of Multi-Axis SMA Array Actuator (a) Substrate board layer with grooves (b) TE module layer (c) Segmentation architecture shown with the heat sink design

VI. Conclusion

A novel compact multi-axis SMA actuator array was developed for driving five-fingered anthropomorphic robot hand. The new actuator array used Segmented Binary Control, which controls the SMA wires segment by segment in a digital manner. SBC simplifies the control of SMA wire but increases the complexity of the design and the number of control loops. A multi-axis segmentation theory was developed to reduce the design complexity and the number of control loops by reducing the number of segments. The segmentation architecture was implemented with ten SMA wires sandwiched between a layer of thermoelectric modules on a printed circuit board and a layer of substrate board with grooves. The substrate board is fabricated using a laser cutter and the process is easily scalable. The fabrication of printed circuit board is also scalable. One of the obstacles to scalable manufacturing of the system is a TE module. A layered manufacturing of TE modules directly on to the substrate board would enable a scalable manufacturing of the whole system and would facilitate customized design of the actuator array.

References

[1] A. Bicchi, "Hands for dexterous manipulation and robust grasping: a difficult road toward simplicity," *Robotics and Automation, IEEE Transactions on*, vol. 16, pp. 652-662, 2000.

[2] J. K. Salisbury and J. J. Craig, "Articulated hands - Force control and kinematic issues," *International Journal of Robotics Research*, vol. 1, pp. 4-17, 1982.

[3] S. C. Jacobsen, J. E. Wood, D. F. Knutti, and K. B. Biggers, "UTAH/MIT DEXTROUS HAND: WORK IN PROGRESS.," in *Robotics Research, the 1st International Symposium.,* 1984.

[4] C. Loucks, V. Johnson, P. Boissiere, G. Starr, and J. Steele, "Modeling and control of the stanford/JPL hand," in *Proc. IEEE Int. Conf. Robotics and Automation. on*, 1987.

[5] T.Iberall, G. Sukhatme, D. Beattie, and G. Bekey, "Control philosophy and simulation of a robotic hand as a model for prosthetic hands," in *Proc. IEEE/RSJ Int. Conf. Intelligent Robots and Systems.*, 1993

[6] A. Caffaz and G. Cannata, "The design and development of the DIST-Hand dexterous gripper," in *Proc. IEEE Int. Conf. Robotics and Automation,* 1998.

[7] H. Kawasaki, T. Komatsu, and K. Uchiyama, "Dexterous anthropomorphic robot hand with distributed tactile sensor: Gifu hand II," *IEEE/ASME Trans. Mechatronics*, vol. 7, pp. 296-303, 2002.

[8] Y. Kuroki, K. Kato, K. Nagasaka, A. Miyamoto, K. Ueno, and J. Yamaguchi, "Motion evaluating system for a small biped entertainment robot," in *Proc. IEEE Int. Conf. Robotics and Automation*, 2004.

[9] Honda Motor Co., Ltd, "Asimo's specification," *Honda Motors*, 2004, <http://world.honda.com/ASIMO/technology/spec.html> (Jan. 2005).

[10] Fujitsu Automation Ltd, "Design Specifations," *Fujitsu Automation*, 2004, <http://www.automation.fujitsu.com/en/products/products09.html> (Jan. 2005)

[11] J. N. Sarris and N. A. Aspragathos, "Development of a simple anthropomorphic robot hand using shape memory alloys," in *IEE Colloquium on Innovative Actuators for Mechatronic Systems*, 1995.

[12] K. Yang and C. L. Gu, "A novel robot hand with embedded shape memory alloy actuators," in *Proc. Institution of Mechanical Engineers, Part C (Journal of Mechanical Engineering Science)*, vol. 216, pp. 737-45, 2002.

[13] T. Okada, "Analysis of Finger Motion and Hand tasks," Biomechanism 3, University of Tokyo press. pp. 133-144, 1975.

[14] M. R. Cutkosky, "On grasp choice, grasp models, and the design of hands for manufacturing tasks," *IEEE Transactions on Robotics and Automation*, vol. 5, pp. 269-79, 1989.

[15] J. Lin, Y. Wu, and T. S. Huang, "Modeling the constraints of human hand motion," in *Workshop on Human Motion*, 7-8 Dec. 2000, Los Alamitos, CA, USA, 2000.

[16] J. Lee and T. L. Kunii, "Model-based analysis of hand posture," *Computer Graphics and Applications, IEEE,* vol. 15, pp. 77-86, 1995.

[17] Y. Wu and T. S. Huang, "Capturing articulated human hand motion: a divide-and-conquer approach," in *Proc. IEEE Int.Conf. Computer Vision*, 1999.

[18] B. Selden, K. Cho, H. Asada, "Segmented Binary Control of Shape Memory Alloy Actuator Systems Using the Peltier Effect, " *in Proc. IEEE Int. Conf. Robotics and Automation*, 2004, pp. 4931-4936

[19] K. J. Cho, H. H. Asada, "Segmentation architecture of multi-axis SMA array actuators inspired by biological muscles," in *Proc. IEEE/RSJ Int. Conf. Intelligent Robots and System*, pp.254-259